J Biomol NMR (2010) 48:49–58
DOI 10.1007/s10858-010-9437-5

ARTICLE

Assessment of GABARAP self-association by its diffusion properties

Victor Pacheco · Peixiang Ma · Yvonne Thielmann · Rudolf Hartmann · Oliver H. Weiergräber · Jeannine Mohrlüder · Dieter Willbold

Received: 20 May 2010 / Accepted: 13 July 2010 / Published online: 28 July 2010

Abstract Gamma-aminobutyric acid type A receptor-associated protein (GABARAP) belongs to a family of small ubiquitin-like adaptor proteins implicated in intracellular vesicle trafficking and autophagy. We have used diffusion-ordered nuclear magnetic resonance spectroscopy to study the temperature and concentration dependence of the diffusion properties of GABARAP. Our data suggest the presence of distinct conformational states and provide support for self-association of GABARAP molecules. Assuming a monomer–dimer equilibrium, a temperature-dependent dissociation constant could be derived. Based on a temperature series of $^{1}H^{15}N$ heteronuclear single quantum coherence nuclear magnetic resonance spectra, we propose residues potentially involved in GABARAP self-interaction. The possible biological significance of these observations is discussed with respect to alternative scenarios of oligomerization.

Keywords Diffusion-ordered spectroscopy · NMR spectroscopy · Protein oligomerization · GABARAP

Electronic supplementary material The online version of this article (doi:10.1007/s10858-010-9437-5) contains supplementary material, which is available to authorized users.

V. Pacheco · P. Ma · Y. Thielmann · R. Hartmann · J. Mohrlüder · D. Willbold (✉)
Institut für Strukturbiologie und Biophysik 3, Forschungszentrum Jülich, 52425 Jülich, Germany
e-mail: d.willbold@fz-juelich.de

O. H. Weiergräber
Institut für Strukturbiologie und Biophysik 2, Forschungszentrum Jülich, 52425 Jülich, Germany

D. Willbold
Institut für Physikalische Biologie und BMFZ, Heinrich-Heine-Universität, 40225 Düsseldorf, Germany

Present Address:
Y. Thielmann
Molecular Membrane Biology, Max Planck Institute of Biophysics, 60438 Frankfurt, Germany

Introduction

The 117 amino acid protein GABARAP was initially isolated by yeast two-hybrid screening, using as bait the long cytoplasmic loop of the $\gamma 2$ subunit of the γ-aminobutyric acid type A receptor ($GABA_A$ receptor, Wang et al. 1999). $GABA_A$ receptors are ligand-gated chloride channels acting as major mediators of fast synaptic inhibition in the central nervous system (Enna and Möhler 2007). They are of particular pharmacological importance and are targeted by numerous drugs used to treat anxiety disorders or to modulate vigilance.

GABARAP is recognized as a versatile adaptor protein implicated in cellular trafficking of the $GABA_A$ receptor, but is also discussed to more generally participate in intracellular vesicular transport, fusion processes and autophagy (Moss and Smart 2001; Kneussel 2002; Kabeya et al. 2004). Nevertheless, the precise molecular mechanisms of its cellular function still remain to be elucidated.

GABARAP is the prototype of a small protein family; in humans the latter includes the following members with sequence identities to GABARAP ranging from 30 to 87%: GEC1 (glandular epithelial cell protein 1), which was characterized as an early estrogen-regulated protein; GATE-16 (Golgi-associated ATPase enhancer of 16 kDa), an essential component of intra-Golgi transport; and LC3 (light chain 3), which is a subunit of microtubule-associated protein complexes. Atg8, the only GABARAP orthologue in yeast, is an

important regulator of autophagosome formation, possibly mediating tethering and hemifusion of membranes upon homo-oligomerization (Nakatogawa et al. 2007).

GABARAP and Atg8, as well as several other members of the GABARAP protein family, have been demonstrated to be enzymatically coupled to a target moiety in a ubiquitin-like modification process (Tanida et al. 2003). In contrast to ubiquitin, which is coupled to various target proteins, GABARAP and Atg8 form conjugates with phosphatidylethanolamine (PE) or phosphatidylserine (PS, Sou et al. 2006). This lipidation is reversible as GABARAP can be cleaved from the lipid by the cysteine protease Atg4B (Tanida et al. 2004).

Detailed structural investigation has yielded crystal structures and nuclear magnetic resonance (NMR) solution structures of GABARAP (Bavro et al. 2002; Coyle et al. 2002; Knight et al. 2002; Stangler et al. 2002; Kuono et al. 2002). Its three-dimensional fold exhibits a ubiquitin-like core with two additional N-terminal α-helices. The N-terminal part of GABARAP is flexible and can adopt multiple conformations (Knight et al. 2002; Stangler et al. 2002). Notably, in one of the published crystal structures, GABARAP forms continuous chains mediated by about ten N-terminal amino acids swapping to the neighbouring molecule (Coyle et al. 2002). A similar mechanism is supported by biochemical studies reporting dimerization of GABARAP (Nymann-Andersen et al. 2002a). Self-interaction involves residues 36–68 of GABARAP, a region that is known to present two hydrophobic pockets termed hp1 and hp2. These are able to engage indole derivatives (Thielmann et al. 2008), apolar side chains of an artificial peptide (Weiergräber et al. 2008) as well as physiological interaction partners such as the $GABA_A$ receptor (Nymann-Andersen et al. 2002b), calreticulin (Mohrlüder et al. 2007a; Thielmann et al. 2009a), the heavy chain of clathrin (Mohrlüder et al. 2007b), the proapoptotic protein Nix (Schwarten et al. 2009) and possibly the N-ethylmaleimide sensitive factor (NSF, Thielmann et al. 2009b). These pockets are lined by side chains of E17, I21, Y25, R28, P30, I32, K48, L50 and F104 for hp1 and by L44, Y49, V51, L55, F60, L63, I64 and R67 for hp2, as determined from crystal structures of GABARAP with an artificial peptide (Weiergräber et al. 2008) and a calreticulin peptide (aa 178–188, Thielmann et al. 2009a). The physiological relevance of GABARAP self-interaction has not been established so far, but it is speculated to be important for the mechanism of $GABA_A$ receptor clustering and trafficking (Nymann-Andersen et al. 2002a).

Studies addressing the physical dimensions of molecules or molecular assemblies have traditionally relied on measurements of the effective radius of gyration by small-angle scattering studies using neutrons or X-rays (Lattman 1994; Kataoka and Goto 1996; Glatter and Kratky 1982). Alternatively, hydrodynamic or Stokes radii have been determined via translational diffusion measurements using dynamic light scattering (Berne and Pecora 2000) or diffusion-ordered spectroscopy (DOSY) NMR (Johnson 1999).

Translational self-diffusion of proteins as measured by DOSY-NMR has been successfully used for the characterization of self-association as well as folding and unfolding processes in solution (Altieri et al. 1995; Dingley et al. 1995; Jones et al. 1997; Pan et al. 1997). Here we applied $^{1}H^{15}N$-DOSY heteronuclear single quantum coherence (HSQC) experiments to study the self-association behaviour of GABARAP in a temperature and concentration dependent manner. In addition, conventional HSQC-NMR spectra reveal residues of GABARAP which may be involved in this process. We propose two alternative modes of GABARAP oligomerization in vivo, which are discussed in light of recent evidence from biochemistry and structural biology.

Materials and methods

Expression and purification of GABARAP

Human GABARAP was expressed in *Escherichia coli* and purified as described previously (Stangler et al. 2001). Uniformly ^{15}N-labelled protein was obtained by growing the bacteria in minimal medium supplemented with ^{15}N-labelled ammonium chloride (Euriso-Top, Saint-Aubin, France) as the sole nitrogen source.

NMR experiments

Measurements were performed on a Varian INOVA 600 MHz spectrometer (Varian, Darmstadt, Germany) operating at 599.644 MHz. Diffusion coefficients were determined by applying the 1D-$^{1}H^{15}N$-DOSY-HSQC pulse sequence (Brand et al. 2007; Wu et al. 1995) without spinning and using a thermostat L900 (Varian) with a temperature accuracy better than 0.1°C. The gradient was calibrated at 25°C with a deuterated methanol sample using diffusion values previously obtained by NMR, for CD_3OH ($D = 2.22 \times 10^{-9}$ m^2/s) and for CHD_2OD ($D = 2.18 \times 10^{-9}$ m^2/s, Holz and Weingärtner 1991). The gradient strength was incremented in 25 steps from 11.2 up to 56.2 G/cm. The following experimental settings were used: diffusion time was 0.2 s, gradient duration was 800 μs and acquisition time was 85 ms. Generally, the highest gradient ratios resulted in a reduction of peak intensities to between three and four percent of their original magnitudes, thus maintaining a clear distinction from background noise. Further details of the procedure are given elsewhere (Johnson 1999; Price 1997, 1998; Antalek

2002; Weingärtner and Holz 2002). The water signal was suppressed with the WATER-GATE sequence. Measurements were performed with 0.05–0.4 mM GABARAP in PBS buffer prepared with a mixture of 10% D_2O and 90% H_2O at pH 7.4 and temperatures between 1 and 35°C. Each experiment was repeated four times, with individual measurements usually agreeing to within 3%. The mean value for each condition, hereafter termed D_{app}, was used in subsequent calculations. Conventional 2D-HSQC experiments were performed with ^{15}N-GABARAP in PBS buffer at concentrations varying from 0.05 to 0.4 mM at temperatures between 2 and 45°C.

The following equation was used to calculate $\Delta\delta_c$, the composite chemical shift perturbation (CSP), which takes into account ^{1}H and ^{15}N chemical shift changes from the HSQC experiments (Thielmann et al. 2008):

$$\Delta\delta_c = \sqrt{[\Delta\delta(^1H)]^2+[\Delta\delta(^{15}N)/5]^2}.$$

Graphics

Molecular graphics were generated using MOLMOL (Koradi et al. 1996); Diagrams were created in Sigma Plot 8.0 (Systat Software Inc., San Jose, USA). Further image processing was done utilizing Adobe Photoshop CS3 (Adobe Systems Inc., San Jose, USA).

Results

GABARAP forms oligomers in solution

Self-association of GABARAP has been shown previously by Nymann-Andersen et al. (2002a). We were able to confirm their observations by photo-induced crosslinking experiments. An SDS polyacrylamide gel of the reaction products is available as supplementary Figure S1. Obviously, dimeric GABARAP fractions can be detected at different temperatures (10, 18, 25°C), with significant variation in quantity. Slight traces of higher order GABARAP oligomers are also visible. To characterize the oligomerization of GABARAP in more detail, NMR spectroscopy was applied.

Temperature and concentration dependence of GABARAP self-association

Diffusion coefficients of GABARAP were measured by ^{1}H^{15}N-DOSY-HSQC with protein concentrations of 50, 100, 200 and 400 μM at temperatures ranging from 1 to 35°C. For every single temperature, the concentration dependence of the apparent diffusion coefficient (D_{app}) can be used for extrapolation to infinite dilution, yielding a quantity termed D_0; according to mass action, the latter corresponds to the limiting case of an entirely monomeric and non-interacting population (for details, refer to supplementary Figure S2 and Table S1). Consequently, the behaviour of D_0 should reflect the structure of monomeric GABARAP whereas D_{app} determined in any real experiment will include various contributions related to protein concentration.

Arrhenius plots provide a convenient means to linearize the temperature dependence of processes governed by activation barriers. Since the viscosity of aqueous solutions approximately obeys an Arrhenius-type law, this type of analysis is applicable to diffusion processes, as well. Interestingly, the Arrhenius plot for D_0 (Fig. 1a) does not show a linear behaviour for the whole temperature range, but exhibits three linear zones with different slopes. Apparent activation energies calculated from these slopes are indicated in the figure. Similar results were obtained for diffusion coefficients measured with 50, 100, 200 and 400 μM GABARAP. The inset in Fig. 1a lists the activation energies calculated for all four concentrations. These values are in the dimension of hydrogen bonding energies. Since concentration-related effects, including oligomerization, should be eliminated by extrapolation to infinite dilution (i.e. in D_0), this behaviour suggests the presence of several distinct conformational states, with transitions occurring around 10 and 22°C, respectively.

The concentration dependence of GABARAP diffusion coefficients is illustrated in Fig. 1b. As expected, we observed a decrease of diffusion coefficients with increasing protein concentration. This is true for the complete temperature range, with the exception of experiments performed at 10 and 22°C (marked by arrows), which only exhibited a slight concentration dependence. Intriguingly, these temperatures coincide with the points of transition in the D_0 Arrhenius plot shown above.

We propose that the concentration-dependent changes of GABARAP diffusion properties are related to formation of a specific oligomer. This conclusion is supported by crosslinking experiments (Nymann-Andersen et al. 2002a, Figure S1). Because the fractions of multimeric species larger than dimers are very small, we choose a simplified model describing solely the monomer–dimer equilibrium, as has been done before (Altieri et al. 1995; Price et al. 1999):

$$M + M \rightleftharpoons D \quad (1)$$

The ^{1}H^{15}N-DOSY-HSQC experiment does not resolve the individual components present in the solution but instead gives a single apparent diffusion coefficient (D_{app}). The latter corresponds to a weighted average of diffusion coefficients of the species involved (monomer and dimer in this case):

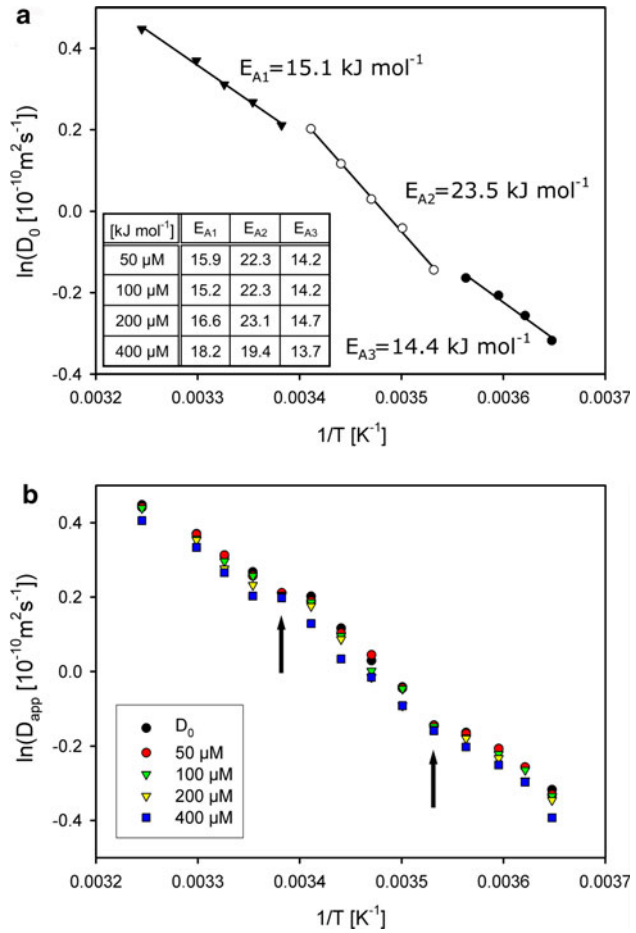

Fig. 1 Arrhenius diagrams showing the temperature dependence of GABARAP's diffusion coefficient. **a** D_0 is the extrapolated diffusion coefficient at infinite dilution. The regression for the logarithm of D_0 reveals three different slopes along the temperature range. The activation energies of diffusion determined from these slopes are indicated; note that the elevated activation energy E_{A2} results in a triphasic Arrhenius plot. This is representative for data measured at all GABARAP concentrations; the corresponding energies are summarized in the inset. **b** Comparison of diffusion coefficients at GABARAP concentrations ranging from infinite dilution to 400 µM. At two distinct temperatures (marked by *arrows*) the variation of diffusion coefficients with concentration is rather small

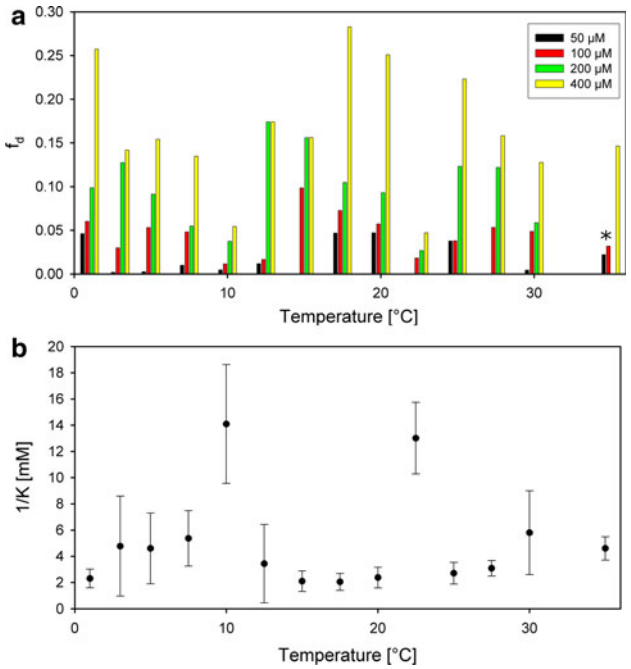

Fig. 2 Illustration of dimer fractions (f_d) and self-dissociation constants of GABARAP. **a** Dimer fraction of GABARAP, depending on temperature and protein concentration (* not determined for 200 µM GABARAP). **b** Self-dissociation constant (mean ± SD) of GABARAP as a function of temperature

$$D_{app} = (1 - f_d)D_m + f_d D_d \quad (2)$$

with f_d the weighting factor for the dimer diffusion coefficient D_d and D_m the diffusion coefficient for the monomer. Since the NMR signal of the dimer should be about twice the signal of a monomer, f_d has to account for mass-averaging of D_m and D_d:

$$f_d = \frac{n_d M_d}{n_m M_m + n_d M_d} = \frac{2n_d}{n_m + 2n_d} = \frac{2n_d}{c} \quad (3)$$

with M_m and M_d the molecular masses and n_m and n_d the number concentrations of monomer and dimer, respectively, and c giving the total concentration of (monomeric) protein molecules in the solution.

Provided the individual diffusion coefficients (D_m and D_d) are known, dimer concentrations can be easily determined from the measured diffusion coefficients (2, 3). Unfortunately, there is no straightforward procedure to calculate D_m under conditions of a real experiment since the concentration-dependence of monomer diffusion is convoluted with the dimerization equilibrium. To circumvent this problem, we make use of a finding reported by Wills and Georgialis (1981), who thoroughly investigated the influence of dimerization on the diffusion properties of bovine pancreatic trypsin inhibitor. They showed that the decrease of diffusion coefficients due to the formation of oligomers strongly outweighs other concentration-dependent effects. With the same rationale, we use the diffusion coefficient at infinite dilution (D_0) as an approximation for D_m which is dependent on temperature, but mostly independent of protein concentration. Assuming spherical molecules, the diffusion coefficient of the dimer can be calculated as $D_d = 0.719\ D_m$ (Wills and Georgialis 1981).

Figure 2a displays the dimer mass fractions (f_d) calculated for the four protein concentrations as a function of temperature. As expected, the dimer fraction increases with the concentration of GABARAP at any given temperature, with a maximum of almost 0.30 at 18°C and 400 µM but barely exceeding 0.05 at the transition temperatures of 10 and 22°C. This is a direct consequence of the weak

concentration dependence of diffusion coefficients at these temperatures. Qualitatively, the behaviour observed here is in good agreement with our crosslinking experiment (Figure S1), which showed the dimer fraction to be very low at 10°C, significantly larger at 18°C and intermediate at 25°C. It should be noted, however, that results obtained by the two methods are not strictly comparable since they measure different quantities: while DOSY-NMR captures an equilibrium distribution, the crosslinking experiment accumulates ternary encounters (protein + protein + crosslinker) during an arbitrary reaction time. From the dimer fraction, monomer and dimer concentrations can be

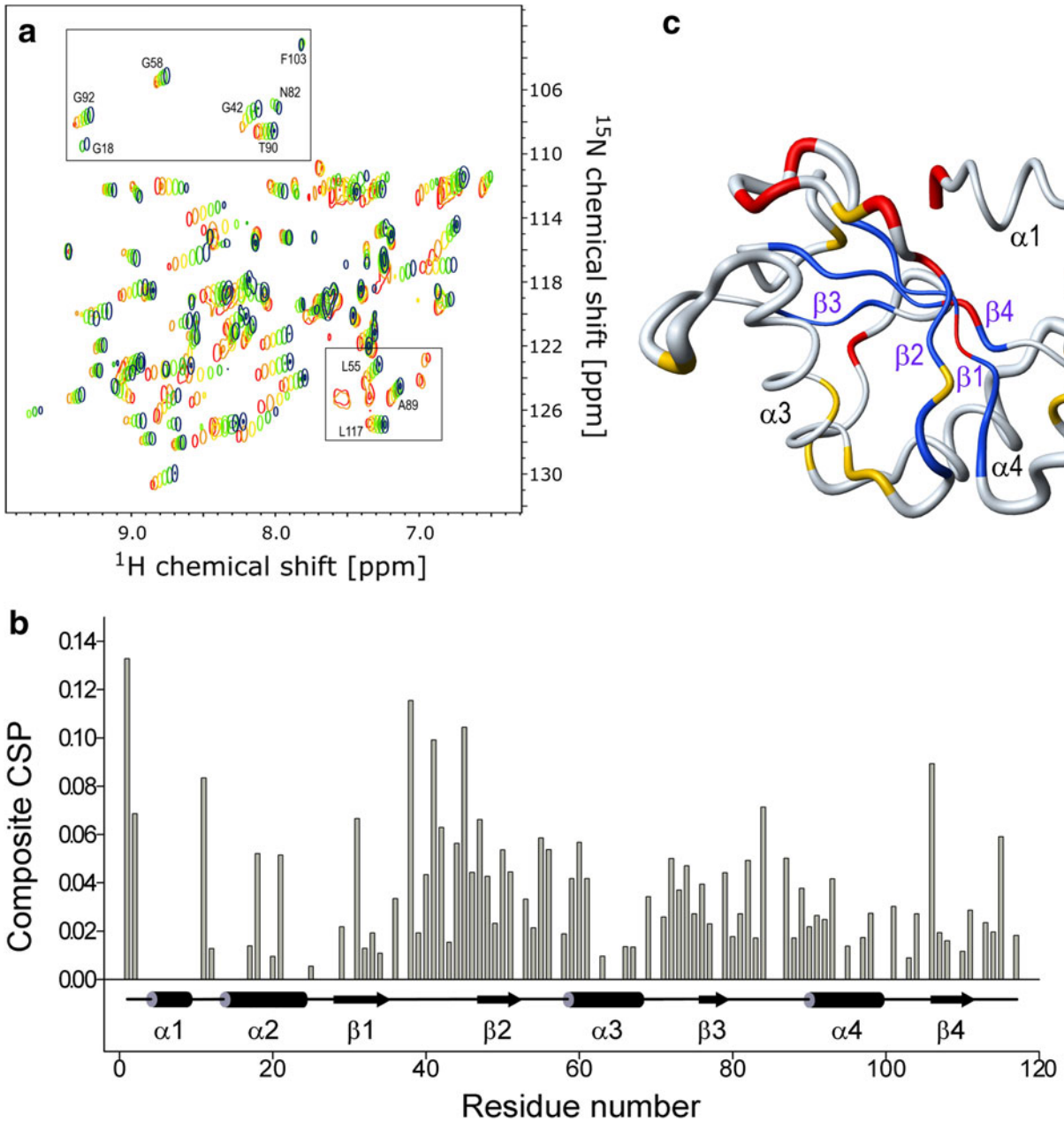

Fig. 3 Impact of temperature changes on the three-dimensional structure of GABARAP. **a** Diagram of a temperature series of $^{1}H^{15}N$-HSQC experiments with 400 μM GABARAP, coloured as follows: *red* 2°C, *orange* 10°C, *yellow* 20°C, *light green* 30°C, *green* 38°C and *blue* 45°C. Two regions revealing discontinuities in signal strength are boxed (see text for details). **b** Composite CSP of clearly identified GABARAP resonances from 10 to 18°C as a function of sequence position. Secondary structure elements are indicated at the bottom. **c** NMR structure of GABARAP (1KOT) in a modified ribbon representation, with the thickness of the trace indicating the spread of the ensemble about the mean structure. Residues rating between 0.05 and 0.06 in composite CSP are highlighted in *yellow*, those exceeding 0.06 in *red*. For ease of orientation, the strands constituting the central *β*-sheet are coloured *blue*

calculated (3), which finally allows for determination of the association constant:

$$K = \frac{n_d}{n_m^2} \quad (4)$$

We have determined K for all temperatures, by averaging over the different protein concentrations (as an equilibrium constant, K should be independent of protein concentration). For convenience, Fig. 2b shows 1/K (the dissociation constant) which is more commonly reported for protein–protein interactions. The dissociation constants derived from the $^{1}H^{15}N$-DOSY-HSQC data generally are in the range between 2 and 6 mM. Exceptions again are the measurements at 10 and 22°C, which give values in the range of 13–14 mM. Thus, our observations indicate a decrease in association tendency of GABARAP around these temperatures.

According to the Stokes–Einstein equation, the apparent diffusion coefficients obtained in our experiments correspond to average hydrodynamic radii ranging from 1.7 to 2.0 nm. The volume of the NMR structure of GABARAP (without a hydration layer) yields a radius of 1.6 nm (volume calculation implemented in http://molbio.info.nih.structbio/basic.html, Richards 1974), thus confirming the lower limit expected for a monomeric population.

Temperature effects on individual GABARAP residues

$^{1}H^{15}N$-HSQC titrations can give valuable information concerning the environment of individual residues while changing physical and chemical parameters. Figure 3a illustrates $^{1}H^{15}N$-HSQC spectra for 400 μM GABARAP recorded at temperatures ranging from 2 to 45°C. Obviously, the protein remains folded over the complete temperature regime and the majority of correlation signals stay well resolved. To identify residues that are affected by the temperature change, the individual chemical shift changes for ^{1}H and ^{15}N between 10 and 18°C were evaluated to yield a composite CSP as described in Materials and methods. These temperatures were chosen because they represent the smallest and largest dimer fraction, respectively, observed in our experiments. The result is shown in Fig. 3b; all residues that exceed a composite CSP of 0.05 are coloured yellow and those exceeding a composite CSP of 0.06 are coloured red in the GABARAP structure depicted in Fig. 3c. These include the N- and C-terminus (M1, K2 and Y115), helices α2 (G18, I21) and α3 (F60), β-strands β1 (V31), β2 (L50) and β4 (Y106) as well as the loops β1β2 (K38, I41, G42, L44, D45, K47), β2α3 (L55, T56), α3β3 (A72) and β3α4 (I84, T87).

It is important to note that for the majority of residues observed in our HSQC experiments, the chemical shifts changed rather smoothly over the temperature range investigated, thus providing little evidence for sharp transitions as suggested by the DOSY-NMR data. However, several resonances were indeed found to disappear or emerge around the proposed transition temperatures, or to form resonance-doublets; some obvious examples are highlighted in Fig. 3a. The first boxed region (upper left) includes signals from G18 and N82, which attain significant magnitude only at elevated temperatures. The opposite is true for the three unassigned resonances in the second box (lower right), which are strongest below 10°C. The latter are likely to correspond to very mobile parts of the structure, most notably helix α1; conformational changes in this region are suspected to play an important role for the biological function of GABARAP, as discussed below.

In the modified ribbon diagram (Fig. 3c), the thickness of the coil represents the spread of the NMR ensemble about the mean structure, which is an indicator of conformational flexibility. It is interesting to note that several residues displaying large CSPs are located in well-defined parts of the structure; significantly, this is true for I21, L50 and F60 lining the hydrophobic pockets on the surface of GABARAP, as well as V31 which resides in close proximity. On the other hand, the N- and C-termini together with the intervening β1β2 loop are inherently much more flexible, but experience additional alterations in structure or dynamics as a function of temperature.

While the composite ($^{1}H^{15}N$) CSP introduced above is a general indicator of changes in the amide environment, its component in the ^{1}H dimension contains information on the type of hydrogen bond involved. Specifically, for protons engaged in intramolecular bonds the ^{1}H CSP is a linear function of temperature with a slope ranging from 0 to -3×10^{-3} ppm/K. On the other hand, if hydrogen bonding interactions between solute and solvent are changed, CSP/ΔT tends to be much larger, usually amounting to -6 to -10×10^{-3} ppm/K (Deslauriers and Smith 1981). Between 10 and 18°C this is the case for M1, K2, F11, V31, K38, K47, T56, A72, N82 and I84. Except for N82, all of these residues had already been identified by the composite CSP calculation.

We conclude that about half of the most significant composite CSPs associated with the temperature shift are indicative of changes in solvation, whereas others provide support for structural changes in the GABARAP molecule.

Discussion

Crosslinking experiments have shown that GABARAP has a tendency to self-associate. The evaluation of the $^{1}H^{15}N$-DOSY-HSQC data as a function of temperature revealed both concentration-independent and -dependent changes in the diffusion properties of GABARAP.

Concentration-independent effects

Analysis of the temperature dependence of D_0 by means of Arrhenius diagrams reveals three linear zones with different slopes. This implies changes in the apparent activation energies of diffusion by about 10 kJ/mol around the transition temperatures of 10 and 22°C, which is in the order of hydrogen bonding energies. Indeed, analysis of conventional HSQC data suggested temperature-dependent changes in hydrogen bonding between GABARAP and solvent for ten amino acids covering the N-terminus, β-strand β1 and several loops, which are likely to reflect conformational changes in the molecule. We therefore speculate that these temperature effects on solvation may modulate the thermodynamics of free diffusion for monomeric GABARAP, as observed in our Arrhenius plots.

Oligomerization of GABARAP

The concentration dependence of diffusion coefficients and their analysis according to a monomer–dimer model, as suggested by crosslinking experiments, allowed for the calculation of dimer fractions and hence self-dissociation constants of GABARAP at the different temperatures. These dissociation constants are in the low millimolar range and comparable to small molecule ligands such as indole derivatives (Thielmann et al. 2008), again with remarkable discontinuities around 10 and 22°C. Taken together, these findings suggest that distinct conformational changes in the GABARAP molecule, which occur as a function of temperature, significantly alter its propensity to form dimers or oligomers. If this is true, should the conventional HSQC analysis reveal more prominent alterations, indicative of a varying extent of protein–protein interaction? We believe this is not necessarily the case, for several reasons: First of all, and most importantly, our calculations indicate that the population of dimeric fractions in solution is relatively low (below 0.3 throughout, and not even exceeding 0.18 for the majority of conditions). Assuming slow exchange between monomeric and dimeric species (relative to the HSQC chemical shift time scale), we might expect appearance of new resonances, which, however, would probably not be detected as significant observations given their reduced height. In the case of rapid exchange, existing peaks would shift in proportion to the dimer fraction, but again, the net effect would be rather small. Second, the $^{1}H^{15}N$ HSQC spectrum mainly reflects the environment of amides and therefore cannot be very sensitive to protein–protein interactions which largely rely on side chain contacts.

The choice of a simple monomer–dimer model for quantitative evaluation of the DOSY-NMR data appears justified in light of the low abundance of larger oligomers in solution (Figure S1). Nevertheless, the physiological environment of GABARAP within the cell may favour the formation of larger oligomers.

Biological relevance of self-association

It is important to note that the temperature dependence of biophysical properties investigated in this study is unlikely to operate as a regulatory mechanism in homoiothermic organisms such as mammals. The sharp decrease of dimerization propensity around 10 and 22°C may thus be considered accidental, reflecting certain properties of the protein surface at non-physiological temperatures.

Irrespective of these considerations, a protein's response to an environmental parameter can be viewed as sampling of the conformational space available to the molecule, and may therefore, to a certain extent, mimic the consequences of physiological stimuli.

Indeed, previous studies have provided evidence for specific conformational changes in proteins of the GABARAP family, which are crucial for biological activity and, at the same time, can be expected to modulate the oligomerization tendency of these molecules. We shall briefly discuss the major findings with relevance to the data presented here.

First of all, the NMR solution structure of GABARAP indicated that the N-terminus can adopt multiple conformations (Stangler et al. 2002). More dramatic alterations were found in one of the crystal structures, where GABARAP forms oligomers in a head-to-tail fashion, placing the first four residues into the hydrophobic pockets of the adjacent molecule (Coyle et al. 2002). Evidence for different conformations of the C-terminus comes from the crystal structures of GATE-16 (Paz et al. 2000) and LC3; the latter has been investigated in a free form and bound to the cysteine protease Atg4B (Sugawara et al. 2004; Satoo et al. 2009). Complex formation with the enzyme leads to a large conformational change of LC3, with the C-terminal residues assuming an extended conformation to access the active centre. Because the amino acids important in this mechanism are conserved, LC3 can be considered a valid model for other family members. While these proteins are tethered to membrane lipids, their C-termini will have to be exposed to some extent, probably resembling the Atg4B-bound form of LC3. The conserved hydrophobic pockets, which constitute the major sites for ligand interaction on GABARAP-family proteins (Weiergräber et al. 2008; Thielmann et al. 2009a; Noda et al. 2008), are also subject to structural alterations. Specifically, engagement of a largely apolar four-amino acid motif found in physiological binding partners (WxxL) induces conformational changes involving helices α2 and α3 as well as adjacent loops (reviewed in Thielmann et al. 2009c; Mohrlüder et al. 2009).

Based on these observations, we propose the following model for the formation of GABARAP dimers or oligomers in solution:

The compact fold of non-lipidated GABARAP, while certainly the prevailing species in solution, is likely to exist in thermal equilibrium with alternate forms in which the N- and/or C-termini are detached from the core domain. This would also provide more spatial freedom to the $\beta1\beta2$ loop, as supported by the HSQC experiments. Similarly, the hydrophobic pockets are clearly able to open up as needed to accommodate large apolar ligand moieties. It is therefore reasonable to envisage an association of GABARAP molecules via the mobilized N-terminus (with its hydrophobic MKFVY sequence) on the one hand and the hp1/hp2 surface on the other. Indeed, such an intermolecular contact has been experimentally discovered in a GABARAP crystal form grown under high-salt conditions (Coyle et al. 2002). In the course of this process an oligomeric chain could form.

The dissociation constants reported in this study are in the low millimolar range and may, at first sight, appear suspicious of merely reflecting unspecific aggregation at high protein concentration. Indeed, while the cellular GABARAP concentration, to our knowledge, has not been determined experimentally, it will certainly be much lower than these dissociation constants, rendering a significant association in the bulk cytosol unlikely. However, these numbers have to be appreciated in the context of the physiological subcellular environment, which clearly differs from a pure protein solution in a test tube. As outlined above, membrane attachment is critical for biological activity of GABARAP and related proteins, and covalent linkage of the C-terminus is expected to destabilize the adjacent N-terminal segment, possibly promoting conformational changes related to oligomerization. Moreover, formation of two-dimensional protein arrays on membrane microdomains may lead to a localized increase in concentration by several orders of magnitude. It is important to note that interactions among membrane-associated GABARAP molecules could occur in two distinct topologies, with individual chains located either on the same membrane (in *cis*) or on different membranes (in *trans*). Support for the latter scenario comes from experiments with yeast Atg8, which has been shown to tether liposomes when conjugated to PE (Nakatogawa et al. 2007). A recent study addressing the specific roles of mammalian GABARAP family members in autophagy suggests that LC3 chiefly promotes phagophore extension, whereas the GABARAP/GATE-16 subfamily is involved in maturation towards a closed autophagosome structure (Weidberg et al. 2010); both processes are likely to involve membrane fusion events. On the molecular level, a number of weak binding instances (e.g. individual GABARAP-GABARAP contacts) may cooperate in generating a significant overall affinity between the membranes hosting these "adhesive" molecules. It is tempting to speculate that this mechanism may also be crucial to other functions of GABARAP in vesicular transport and sorting, most notably in the secretory pathway.

Conclusion

Current evidence suggests that self-association may constitute an important functional property of GABARAP-family proteins. In the present work, we have investigated the oligomerization of soluble GABARAP, yielding the first quantitative assessment of this process. While our results are consistent with and provide an extension to available structural and functional data, several issues still need to be resolved. These include the precise biological role(s) of GABARAP in its cellular environment, which will help us appreciate the significance of self-association in the physiological context. We hope that this contribution will inspire new experiments further elucidating the biochemistry and cell biology of this exciting family of adaptor proteins.

Acknowledgments O. H. Weiergräber is grateful to Georg Büldt for continuous generous support. V. Pacheco appreciates support by Heike Schneider. This work was supported by a Deutsche Forschungsgemeinschaft (DFG) grant to D. W. (Wi1472/5) and a PhD scholarship from the Deutscher Akademischer Austauschdienst (DAAD) to P. M.

References

Altieri AS, Hinton DP, Byrd RA (1995) Association of biomolecular systems via pulsed field gradient NMR self diffusion measurements. J Am Chem Soc 117:7566–7567

Antalek B (2002) Using pulsed gradient spin echo NMR for chemical mixtures analysis: How to obtain optimal results. Concepts Magn Reson 14:225–258

Bavro VN, Sola M, Bracher A, Kneussel M, Betz H, Weissenhorn W (2002) Crystal structure of the $GABA_A$-receptor-associated protein, GABARAP. EMBO Rep 3:183–189

Berne BJ, Pecora R (2000) Dynamic light scattering with applications to chemistry, biology and physics. Dover Publications, New York

Brand T, Cabrita EJ, Morris GA, Günther R, Hofmann HJ, Berger S (2007) Residue-specific NH exchange rates studied by NMR diffusion experiments. J Magn Reson 187:97–104

Coyle JE, Qamar S, Rajashankar KR, Nikolov DB (2002) Structure of GABARAP in two conformations: implications for $GABA_A$ receptor localization and tubulin binding. Neuron 33:63–74

Deslauriers R, Smith CP (1981) The multinuclear NMR approach to peptides: structures, conformations, and dynamics. In: Berliner JL, Reuben J (eds) Biological magnetic resonance. Plenum Press, New York, pp 243–344

Dingley AJ, Mackay JP, Chapman BE, Morris MB, Kuchel PW, Hambly BD, King GF (1995) Measuring protein self-association using pulsed-field-gradient NMR spectroscopy: application to myosin light chain 2. J Biomol NMR 6:321–328

Enna SJ, Möhler H (2007) The GABA receptors, 3rd edn. Humana Press, Totowa

Glatter O, Kratky O (1982) Small angle X-ray scattering. Academic Press, London

Holz M, Weingärtner H (1991) Calibration in accurate spin-echo self-diffusion measurements using ^{1}H and less-common nuclei. J Magn Reson 92:115–125

Johnson CS Jr (1999) Diffusion ordered nuclear magnetic resonance spectroscopy: principles and applications. Prog Nucl Magn Reson Spectrosc 34:203–256

Jones JA, Wilkins DK, Smith LJ, Dobson CM (1997) Characterisation of protein unfolding by NMR diffusion measurements. J Biomol NMR 10:199–203

Kabeya Y, Mizushima N, Yamamoto A, Oshitani-Okamoto S, Ohsumi Y, Yoshimori T (2004) LC3, GABARAP and GATE16 localize to autophagosomal membrane depending on form-II formation. J Cell Sci 117:2805–2812

Kataoka M, Goto Y (1996) X-ray solution scattering studies of protein folding. Fold Des 1:R107–R114

Kneussel M (2002) Dynamic regulation of $GABA_A$ receptors at synaptic sites. Brain Res Rev 39:74–83

Knight D, Harris R, McAlister MS, Phelan JP, Geddes S, Moss SJ, Driscoll PC, Keep NH (2002) The X-ray crystal structure and putative ligand-derived peptide binding properties of gamma-aminobutyric acid receptor type A receptor-associated protein. J Biol Chem 277:5556–5561

Koradi R, Billeter M, Wüthrich K (1996) MOLMOL: a program for display and analysis of macromolecular structures. J Mol Graph 14:51–55

Kuono T, Miura K, Kanematsu T, Shirakawa M, Hirata M, Kawano K (2002) ^{1}H, ^{13}C and ^{15}N resonance assignments of GABARAP, $GABA_A$ receptor associated protein. J Biomol NMR 22:97–98

Lattman EE (1994) Small angle scattering studies of protein folding. Curr Opin Struct Biol 4:87–92

Mohrlüder J, Stangler T, Hoffmann Y, Wiesehan K, Mataruga A, Willbold D (2007a) Identification of calreticulin as a ligand of GABARAP by phage display screening of a peptide library. FEBS J 274:5543–5555

Mohrlüder J, Hoffmann Y, Stangler T, Hänel K, Willbold D (2007b) Identification of clathrin heavy chain as a direct interaction partner for the γ-aminobutyric acid type A receptor associated protein. Biochemistry 46:14537–14543

Mohrlüder J, Schwarten M, Willbold D (2009) Structure and possible function of gamma-aminobutyrate type A receptor-associated protein. FEBS J 276:4989–5005

Moss SJ, Smart TG (2001) Constructing inhibitory synapses. Nat Rev Neurosci 2:240–250

Nakatogawa H, Ichimura Y, Ohsumi Y (2007) Atg8, a ubiquitin-like protein required for autophagosome formation, mediates membrane tethering and hemifusion. Cell 130:165–178

Noda NN, Kumeta H, Nakatogawa H, Satoo K, Adachi W, Ishii J, Fujioka Y, Ohsumi Y, Inagaki F (2008) Structural basis of target recognition by Atg8/LC3 during selective autophagy. Genes Cells 13:1211–1218

Nymann-Andersen J, Wang H, Olsen RW (2002a) Biochemical identification of the binding domain in the $GABA_A$ receptor-associated protein (GABARAP) mediating dimer formation. Neuropharmacology 43:476–481

Nymann-Andersen J, Wang H, Chen L, Kittler JT, Moss SJ, Olsen RW (2002b) Subunit specificity and interaction domain between $GABA_A$ receptor-associated protein (GABARAP) and $GABA_A$ receptors. J Neurochem 80:815–823

Pan H, Barany G, Woodward C (1997) Reduced BPTI is collapsed. A pulsed field gradient NMR study of unfolded and partially folded bovine pancreatic trypsin inhibitor. Protein Sci 6: 1985–1992

Paz Y, Elazar Z, Fass D (2000) Structure of GATE-16, membrane transport modulator and mammalian ortholog of autophagocytosis factor Aut7p. J Biol Chem 275:25445–25450

Price WS (1997) Pulsed-field gradient nuclear magnetic resonance as a tool for studying translational diffusion: Part I. Basic Theory. Concepts Magn Reson 9:299–336

Price WS (1998) Pulsed-field gradient nuclear magnetic resonance as a tool for studying translational diffusion: Part II. Experimental aspects. Concepts Magn Reson 10:197–237

Price WS, Tsuchiya F, Arata Y (1999) Lysozyme aggregation and solution properties studied using PGSE NMR diffusion measurements. J Am Chem Soc 121:11503–11512

Richards FM (1974) The interpretation of protein structures: total volume, group volume distributions and packing density. J Mol Biol 82:1–14

Satoo K, Noda NN, Kumeta H, Fujioka Y, Ohsumi Y, Inagaki F (2009) The structure of Atg4B-LC3 complex reveals the mechanism of LC3 processing and delipidation during autophagy. EMBO J 28:1341–1350

Schwarten M, Mohrlüder J, Ma P, Stoldt M, Thielmann Y, Stangler T, Hersch N, Hoffmann B, Merkel R, Willbold D (2009) Nix directly binds to GABARAP: a possible crosstalk between apoptosis and autophagy. Autophagy 5:690–698

Sou YS, Tanida I, Komatsu M, Ueno T, Kominami E (2006) Phosphatidylserine in addition to phosphatidylethanolamine is an in vitro target of the mammalian Atg8 modifiers, LC3, GABARAP, and GATE-16. J Biol Chem 281:3017–3024

Stangler T, Mayr LM, Dingley AJ, Luge C, Willbold D (2001) Sequence-specific ^{1}H, ^{13}C and ^{15}N resonance assignments of human GABA receptor associated protein. J Biomol NMR 21: 183–184

Stangler T, Mayr LM, Willbold D (2002) Solution structure of human $GABA_A$ receptor-associated protein GABARAP: implications for biological function and its regulation. J Biol Chem 277: 13363–13366

Sugawara K, Suzuki NN, Fujioka Y, Mizushima N, Ohsumi Y, Inagaki F (2004) The crystal structure of microtubule-associated protein light chain 3, a mammalian homologue of Saccharomyces cerevisiae Atg8. Genes Cells 9:611–618

Tanida I, Komatsu M, Ueno T, Kominami E (2003) GATE-16 and GABARAP are authentic modifiers mediated by Apg7 and Apg3. Biochem Biophys Res Commun 300:637–644

Tanida I, Sou YS, Ezaki J, Minematsu-Ikeguchi N, Ueno T, Kominami E (2004) HsAtg4B/HsApg4B/autophagin-1 cleaves the carboxyl termini of three human Atg8 homologues and delipidates microtubule-associated protein light chain 3- and $GABA_A$ receptor-associated protein-phospholipid conjugates. J Biol Chem 279:36268–36276

Thielmann Y, Mohrlüder J, Koenig BW, Stangler T, Hartmann R, Becker K, Höltje H-D, Willbold D (2008) An indole-binding site is a major determinant of the ligand specificity of the GABA type A receptor-associated protein GABARAP. ChemBioChem 11:1767–1775

Thielmann Y, Weiergräber OH, Mohrlüder J, Willbold D (2009a) Structural framework of the GABARAP-calreticulin interface–implications for substrate binding to endoplasmic reticulum chaperones. FEBS J 276:1140–1152

Thielmann Y, Weiergräber OH, Ma P, Schwarten M, Mohrlüder J, Willbold D (2009b) Comparative modeling of human NSF reveals a possible binding site for GABARAP and GATE-16. Proteins 77:637–646

Thielmann Y, Weiergräber OH, Mohrlüder J, Willbold D (2009c) Structural characterization of GABARAP-ligand interactions. Mol Biosyst 5:575–579

Wang H, Bedford FK, Brandon NJ, Moss SJ, Olsen RW (1999) $GABA_A$-receptor-associated protein links $GABA_A$ receptors and the cytoskeleton. Nature 397:69–72

Weidberg H, Shvets E, Shpilka T, Shimron F, Shinder V, Elazar Z (2010) LC3 and GATE-16/GABARAP subfamilies are both

essential yet act differently in autophagosome biogenesis. EMBO J 29:1792–1802

Weiergräber OH, Stangler T, Thielmann Y, Mohrlüder J, Wiesehan K, Willbold D (2008) Ligand binding mode of $GABA_A$ receptor-associated protein. J Mol Biol 381:1320–1331

Weingärtner H, Holz M (2002) NMR studies of self-diffusion in liquids. Annu Rep Prog Chem Sect C 98:121–155

Wills PR, Georgialis Y (1981) Concentration dependence of the diffusion coefficient of a dimerizing protein: bovine pancreatic trypsin inhibitor. J Phys Chem 85:3978–3984

Wu D, Chen A, Johnson CS Jr (1995) An improved diffusion-ordered spectroscopy experiment incorporating bipolar-gradient pulses. J Magn Reson A115:260–264